IET Signal Processing

Research Article

IET Journals
The Institution of Engineering and Technology

Reconstruction of uniformly sampled signals from non-uniform short samples in fractional Fourier domain

ISSN 1751-9675
Received on 31st July 2014
Revised on 20th September 2015
Accepted on 7th October 2015
doi: 10.1049/iet-spr.2015.0061
www.ietdl.org

Yang Hu[1], Feng Zhang[1] ✉, Liyun Xu[2], Ran Tao[1,2], Yue Wang[1,2]

[1]*Department of Electronic Engineering, Beijing Institute of Technology, Beijing 100081, People's Republic of China*
[2]*School of Mathematics and Statistics, Beijing Institute of Technology, Beijing 100081, People's Republic of China*
✉ *E-mail: ouo@bit.edu.cn*

Abstract: Signal reconstruction from non-uniform samples, especially for non-stationary signals, is an important issue in the area of digital signal processing. As a type of signal processing tool, the fractional Fourier transform has been proved to be effective for solving problems in non-stationary signal processing. For non-stationary discrete-time signals, the reconstruction of uniformly sampled signals from non-uniform samples in the fractional Fourier domain is first derived in this study. Since only finite non-uniform samples are collected in practical applications, for preferable reconstruction, two types of symmetric extensions are considered in the reconstruction to overcome the discontinuity problem that exists in the periodisation of short non-stationary sequences, which is more critical than that of long sequences. In addition, the average signal-to-noise ratio is used to evaluate the performance of the reconstruction with two types of symmetric extensions. Simulations and two applications are given to verify the effectiveness of the proposed reconstruction method.

1 Introduction

Non-stationary signal processing, such as the processing of gravity waves, broad-band chirp signals and radar signals, plays a fundamental role in the area of modern digital signal processing [1, 2]. As the classical Fourier transform (FT) is not suitable for analysing and processing non-stationary signals, many useful tools have been introduced, such as the short-time Fourier transform, wavelet transform, fractional FT (FRFT) and linear canonical transform (LCT) [3–7]. Among all of these processing tools, FRFT can be interpreted as a rotation of FT by an angle α in the time–frequency plane and serves as an orthonormal signal representation for chirp signals [3, 4]. Compared with FT, FRFT is more flexible and suitable for processing non-stationary signals due to an additional degree of freedom. The advantage of using FRFT is that a traditional non-bandlimited signal in the Fourier domain may be bandlimited in the fractional Fourier domain (FRFD) for a certain value of an angle α. Therefore, FRFT has become the focus of many research papers in recent years and has been widely applied in signal processing [8, 9], such as filtering in the FRFD, chirp signal detection and estimation, and the analysis of long range dependence in a time series.

Most of the above-mentioned applications in the FRFD always assume that the digital signal is obtained by sampling an analogue signal at uniform time intervals. The uniform sampling theorem for a bandlimited signal in the FRFD states that the original signal can be reconstructed from the uniform samples in the FRFD when the sampling interval satisfies the uniform sampling conditions [10, 11]. However, these conditions may not be satisfied by the current monolithic analogue-to-digital converter technologies. Non-uniform sampling usually occurs in the data acquisition systems due to an imperfect timebase or random events [12, 13]. Due to the errors that result from non-uniform sampling are usually dominating and cannot be ignored in non-stationary signal processing, reconstruction techniques associated with non-uniformly sampled signals should be developed. Although the spectral analysis of non-uniformly sampled signals in the FRFD and some reconstruction methods of bandlimited signals in the linear canonical domain has been reported so far [14–19], no results regarding the reconstruction of uniformly sampled signals from non-uniform samples in the FRFD have been published yet. It is therefore worthwhile and interesting to research this type of reconstruction in the FRFD.

In this paper, the reconstruction of a uniformly sampled sequence from a non-uniformly sampled sequence in the FRFD is proposed. Specifically, our work is effective for short non-stationary sequences. The paper is organised as follows. In Section 2, we review the definitions of the FRFT, fractional Fourier series (FRFS) and discrete FRFT (DFRFT). In Section 3, the formula of reconstructing the DFRFT of a uniformly sampled sequence from that of a non-uniformly sampled sequence is derived when the sampling time offsets are known. By taking the inverse transform of the obtained DFRFT, the uniformly sampled sequence can be reconstructed. Moreover, based on the equivalence between the DFRFT of a finite sequence and the FRFS of its periodically extended sequence, we consider two types of symmetric extensions to eliminate a discontinuity problem and reduce the high-frequency contents in the FRFD. Simulations and two applications are given to verify the validity of the proposed method in Section 4. Finally, we make a conclusion in Section 5.

2 Definition of the FRFT, FRFS and DFRFT

The FRFT of a signal $f(t)$ with angle α is defined as [1, 3]

$$F^{\alpha}(u) = F^{\alpha}[f(t)](u) = \int_{-\infty}^{\infty} K_{\alpha}(u, t) f(t)\, \mathrm{d}t, \tag{1}$$

where the transform kernel is

$$K_{\alpha}(u, t) = \begin{cases} A_{\alpha} \exp\left(\mathrm{j}(u^2/2)\cot\alpha - \mathrm{j}ut\csc\alpha + \mathrm{j}(t^2/2)\cot\alpha\right), & \alpha \neq k\pi \\ \delta(t-u), & \alpha = 2k\pi \\ \delta(t+u), & \alpha = (2k+1)\pi \end{cases}, \tag{2}$$

$$A_{\alpha} = \sqrt{\frac{1 - \mathrm{j}\cot\alpha}{2\pi}}.$$

When the angle is $\alpha = \pi/2$, FRFT degenerates to FT. It should be

IET Signal Process., 2016, Vol. 10, Iss. 2, pp. 140–149

noted that when $\alpha = k\pi$, the FRFT of a signal is the signal $f(u)$ or $f(-u)$, which is of no particular interest. Thus, we only consider the case of $\alpha \neq k\pi$. Without loss of generality, we assume $0 < \alpha < \pi$ in this paper. The FRFT can be regarded as expressing $f(t)$ on a basis formed by the set of functions $K_\alpha(u, t)$, so the FRFT of a chirp signal with a proper angle is an impulse. If the chirp rate of the signal is μ_0, the proper angle is $\alpha_0 = \operatorname{arc\,cot}(-\mu_0)$ which is called the matched-angle. A signal $f(t)$ is called a Ω_α bandlimited signal in the FRFT sense [10, 11], when

$$F^\alpha(u) = 0, \quad \text{for} \quad |u| > \Omega_\alpha, \tag{3}$$

where Ω_α is called the bandwidth (or the infimum) of the signal $f(t)$ in the FRFD.

The FRFT of the uniformly sampled signal with sampling interval Δt is [1, 3, 15]

$$\begin{aligned} \breve{F}^\alpha(u) &= F^\alpha\left[\sum_{n=-\infty}^{\infty} f(n\Delta t)\delta(t - n\Delta t)\right](u) \\ &= \int_{-\infty}^{\infty} K_\alpha(u, t) \sum_{n=-\infty}^{\infty} f(n\Delta t)\delta(t - n\Delta t)\, \mathrm{d}t \\ &= \frac{1}{\Delta t} e^{\mathrm{j}(u^2/2)\cot\alpha} \sum_{n=-\infty}^{\infty} F^\alpha\left(u - n\frac{2\pi \sin\alpha}{\Delta t}\right) \\ &\quad \times e^{-\mathrm{j}(1/2)\cot\alpha(u - n(2\pi\sin\alpha/\Delta t))^2}. \end{aligned} \tag{4}$$

Equation (4) shows that the FRFT of the uniformly sampled signal replicates $F^\alpha(u)$ with a period of $2\pi\sin\alpha/\Delta t$ with linear phase modulation. In this case, $\breve{F}^\alpha(u)$ satisfies

$$\begin{aligned} &\breve{F}^\alpha\left(u - \frac{2\pi\sin\alpha}{\Delta t}\right) \mathrm{e}^{-j(1/2)(u - (2\pi\sin\alpha/\Delta t))^2 \cot\alpha} \\ &\quad = \breve{F}^\alpha(u) \mathrm{e}^{-j(u^2/2)\cot\alpha}, \end{aligned} \tag{5}$$

which is called the chirp-periodicity of angle α. Similarly, by sampling in the FRFD with sampling interval $\Delta\tau$, the inverse FRFT is

$$\begin{aligned} \widehat{f}(t) &= \int_{-\infty}^{\infty} K_{-\alpha}(u, t) \sum_{m=-\infty}^{\infty} F^\alpha(m\Delta\tau)\delta(u - m\Delta\tau)\, \mathrm{d}u \\ &= \mathrm{e}^{-j(t^2/2)\cot\alpha} \sum_{m=-\infty}^{\infty} f\left(t - m\frac{2\pi\sin\alpha}{\Delta\tau}\right) \\ &\quad \times \mathrm{e}^{j(1/2)\cot\alpha(t - m(2\pi\sin\alpha/\Delta\tau))^2}. \end{aligned} \tag{6}$$

Equation (6) indicates that the continuous-time signal $\widehat{f}(t)$ can be chirp periodic by sampling in the FRFD. Thus, $\widehat{f}(t)$ satisfies

$$\widehat{f}\left(t - \frac{2\pi\sin\alpha}{\Delta\tau}\right) \mathrm{e}^{j(1/2)(t - (2\pi\sin\alpha/\Delta\tau))^2 \cot\alpha} = \widehat{f}(t) \mathrm{e}^{j(t^2/2)\cot\alpha}.$$

As one scheme of the fractional Fourier analysis method, the FRFS is the generalisation of the Fourier series (FS). It is defined as

$$\widehat{f}(t) = \mathrm{e}^{-j(1/2)\cot\alpha \cdot t^2} \sum_{m=-\infty}^{\infty} F_m^\alpha \mathrm{e}^{-j(1/2)\cot\alpha(m\Delta\tau)^2} \mathrm{e}^{j(1/\sin\alpha)m\Delta\tau \cdot t}, \tag{7}$$

where F_m^α are the FRFS coefficients of $\widehat{f}(t)$. More detailed work on the FRFS can be found in [7].

By sampling uniformly N points in the replicated period $2\pi\sin\alpha/\Delta t$ in the FRFD, the sampling interval Δu in the FRFD is $\Delta u = 2\pi\sin\alpha/(N\Delta t)$. Thus, the DFRFT of the discrete-time signal $f[n]$ can be defined as [3, 16]

$$F^\alpha[m] = \mathrm{A}_\alpha \mathrm{e}^{j(1/2)\cot\alpha m^2 \Delta u^2} \sum_{n \in \langle N \rangle} f[n] \mathrm{e}^{j(1/2)\cot\alpha n^2 \Delta t^2 - j(2\pi/N)mn}, \tag{8}$$

where $\langle N \rangle$ denotes the interval $[0, 1, \ldots, N-1]$ without loss of generality. Then, the inverse DFRFT can be defined as

$$f[n] = \frac{1}{N\mathrm{A}_\alpha} \mathrm{e}^{-j(1/2)\cot\alpha n^2 \Delta t^2} \sum_{m \in \langle N \rangle} F^\alpha[m] \mathrm{e}^{-j(1/2)\cot\alpha m^2 \Delta u^2 + j(2\pi/N)mn}. \tag{9}$$

The conventional time-bandwidth product $(1/\Delta f) \cdot (1/\Delta t) = (2\pi/\Delta\Omega) \cdot (1/\Delta t) = N$ is the minimum number of samples to identify a signal whose energy is confined to $1/\Delta f$ and $1/\Delta t$ in the time domain and the frequency domain, respectively. Likewise, the product $(2\pi\sin\alpha/\Delta u) \cdot (\sin\alpha/\Delta t) \cdot (1/\sin\alpha) = N$ is the minimum number of samples to identify a signal whose energy is confined to $2\pi\sin\alpha/\Delta u$ and $\sin\alpha/\Delta t$ in the time domain and the FRFD, respectively. This minimum sample number N is also referred to as the number of freedom degrees.

3 Reconstruction of uniform samples from non-uniform samples in the FRFD

Non-uniform sampling occurs in a broad range of applications due to imperfect timebase or random events. The properties and applications of non-uniform sampling in the traditional Fourier domain have been extensively studied [20–23], especially the reconstruction of uniformly sampled signals from non-uniformly sampled signals. However, these works on recurrent non-uniform sampling often consider sampling of relatively long signals, because the reconstruction functions have infinite length and the reconstruction methods require infinite data sets theoretically. This may be not feasible in applications because the numerical implementation of the reconstruction methods always needs finite data. Moreover, these existing results are only suitable for bandlimited signals and may obtain incorrect results for non-bandlimited signals in the Fourier domain. Due to the fact that the non-bandlimited signals in the Fourier domain may be bandlimited in the FRFD, we present the reconstruction of a uniformly sampled sequence from a non-uniformly sampled sequence in the FRFD in this section. Moreover, the non-uniform sampling pattern considered here is not the recurrent non-uniform sampling and the proposed reconstruction method is suitable for short transient sequences.

3.1 Relationship between uniform samples and non-uniform samples in the FRFD

Let the signal $f(t)$ be a continuous-time signal with its FRFT $F^\alpha(u)$ bandlimited to $(-\Omega_\alpha, \Omega_\alpha)$ in the αth FRFD. Its uniformly sampled sequence is $f[n]$ for $n = 0, 1, 2, \ldots, N-1$. Therefore, the DFRFT of $f[n]$ is given by

$$F^\alpha[m] = \mathrm{A}_\alpha \mathrm{e}^{j(1/2)\cot\alpha m^2 \Delta u^2} \sum_{n=0}^{N-1} f[n] \mathrm{e}^{j(1/2)\cot\alpha n^2 \Delta t^2 - j(2\pi/N)mn}, \tag{10}$$

where Δt and Δu are the sampling interval in the time domain and the FRFD, respectively. Similarly, the inverse DFRFT is

$$f[n] = \frac{1}{N\mathrm{A}_\alpha} \mathrm{e}^{-j(1/2)\cot\alpha n^2 \Delta t^2} \sum_{m=0}^{N-1} F^\alpha[m] \mathrm{e}^{-j(1/2)\cot\alpha m^2 \Delta u^2 + j(2\pi/N)mn}. \tag{11}$$

By non-uniformly sampling $f(t)$ at $t_n = (n + a_n)\Delta t$, we can obtain a discrete-time signal $\tilde{f}[n]$, where Δt is the sampling interval and a_n

are sampling time offsets for $n = 0, 1, 2, \ldots, N-1$. The DFRFT of $\tilde{f}[n]$ is given by

$$\tilde{F}^{\alpha}[m] = \mathrm{A}_{\alpha} \mathrm{e}^{j(1/2)\cot\alpha m^2 \Delta u^2} \sum_{n=0}^{N-1} \tilde{f}[n] \mathrm{e}^{j(1/2)\cot\alpha n^2 \Delta t^2 - j(2\pi/N)mn}. \quad (12)$$

Simultaneously, utilising (11), $\tilde{f}[n]$ can be represented as

$$\begin{aligned} \tilde{f}[n] = f[n + a_n] = \frac{1}{N\mathrm{A}_{\alpha}} \mathrm{e}^{-j(1/2)\cot\alpha(n+a_n)^2 \Delta t^2} \\ \sum_{m=0}^{N-1} F^{\alpha}[m] \mathrm{e}^{-j(1/2)\cot\alpha m^2 \Delta u^2 + j(2\pi/N)m(n+a_n)}. \end{aligned} \quad (13)$$

Substituting (13)into (12), we can deduce that

$$\begin{aligned} \tilde{F}^{\alpha}[k] &= \frac{1}{N} \sum_{m=0}^{N-1} \sum_{n=0}^{N-1} \mathrm{e}^{(j/2)\cot\alpha(k^2 - m^2)\Delta u^2} \mathrm{e}^{-j(2\pi/M)(nk - m(n+a_n))} \\ &\quad \cdot \mathrm{e}^{-(j/2)\cot\alpha(2na_n + a_n^2)\Delta t^2} F^{\alpha}[m] \\ &= \frac{1}{N} \mathrm{e}^{(j/2)\cot\alpha k^2 \Delta u^2} \sum_{m=0}^{N-1} \sum_{n=0}^{N-1} \mathrm{e}^{-j(2\pi/M)(nk - m(n+a_n))} \\ &\quad \cdot \mathrm{e}^{-(j/2)\cot\alpha(2na_n + a_n^2)\Delta t^2} \mathrm{e}^{-(j/2)\cot\alpha m^2 \Delta u^2} F^{\alpha}[m] \\ &= \mathrm{e}^{(j/2)\cot\alpha k^2 \Delta u^2} \sum_{m=0}^{N-1} B[m, (k-m) \bmod N] \\ &\quad \mathrm{e}^{-(j/2)\cot\alpha m^2 \Delta u^2} F^{\alpha}[m], \end{aligned} \quad (14)$$

where

$$B[m, k] = \frac{1}{N} \sum_{n=0}^{N-1} \mathrm{e}^{j(2\pi/N)\cdot m \cdot a_n} \mathrm{e}^{-(j/2)\cot\alpha(2na_n + a_n^2)\Delta t^2} \mathrm{e}^{-j(2\pi/N)nk}$$

The notation $B[m, k]$ can be regarded as the discrete FT of $\mathrm{e}^{j(2\pi/N)ma_n - (j/2)\cot\alpha(2na_n + a_n^2)\Delta t^2}$ multiplied by a constant.

By rewriting (14) in a matrix form, we have

$$\tilde{\boldsymbol{F}}^{\alpha} = \boldsymbol{A} \cdot \boldsymbol{B} \cdot \boldsymbol{C} \cdot \boldsymbol{F}^{\alpha}, \quad (15)$$

where the matrices are defined as follows

$$\boldsymbol{A} = \mathrm{diag}\left[\mathrm{e}^{\frac{j}{2}\cot\alpha \cdot \Delta u^2 \cdot 0}, \mathrm{e}^{\frac{j}{2}\cot\alpha \cdot \Delta u^2 \cdot 1^2}, \mathrm{e}^{\frac{j}{2}\cot\alpha \cdot \Delta u^2 \cdot 2^2}, \ldots, \mathrm{e}^{\frac{j}{2}\cot\alpha \cdot \Delta u^2 \cdot (N-1)^2}\right],$$

$$\boldsymbol{B} = \begin{bmatrix} B[0,0] & B[1,N-1] & \cdots & B[N-2,2] & B[N-1,1] \\ B[0,1] & B[1,0] & \cdots & B[N-2,3] & B[N-1,2] \\ \vdots & \vdots & \ddots & \vdots & \vdots \\ B[0,N-2] & B[1,N-3] & \cdots & B[N-2,0] & B[N-1,N-1] \\ B[0,N-1] & B[1,N-2] & \cdots & B[N-2,1] & B[N-1,0] \end{bmatrix},$$

$$\boldsymbol{C} = \mathrm{diag}\left[\mathrm{e}^{-(j/2)\cot\alpha \cdot \Delta u^2 \cdot 0}, \mathrm{e}^{-(j/2)\cot\alpha \cdot \Delta u^2 \cdot 1^2}, \mathrm{e}^{-(j/2)\cot\alpha \cdot \Delta u^2 \cdot 2^2}, \ldots, \mathrm{e}^{-(j/2)\cot\alpha \cdot \Delta u^2 \cdot (N-1)^2}\right],$$

$$\tilde{\boldsymbol{F}}^{\alpha} = \left[\tilde{F}^{\alpha}[0], \tilde{F}^{\alpha}[1], \tilde{F}^{\alpha}[2], \ldots, \tilde{F}^{\alpha}[N-1]\right]^{\mathrm{T}},$$

and

$$\boldsymbol{F}^{\alpha} = [F^{\alpha}[0], F^{\alpha}[1], F^{\alpha}[2], \ldots, F^{\alpha}[N-1]]^{\mathrm{T}},$$

where diag stands for the diagonal matrix with the column vector on its diagonal and the superscript T indicates matrix transposition. Equation (15) introduces a simple relationship between the DFRFT of a non-uniformly sampled sequence and the DFRFT of a uniformly sampled sequence. It shows that matrix $\boldsymbol{B}$ is not a function of $f[n]$, which is useful for the reconstruction of a uniformly sampled signal in the FRFD. From (15), the DFRFT of a uniformly sampled sequence can be obtained by the following equation

$$\boldsymbol{F}^{\alpha} = \boldsymbol{C}^{-1} \cdot \boldsymbol{B}^{-1} \cdot \boldsymbol{A}^{-1} \cdot \tilde{\boldsymbol{F}}^{\alpha}. \quad (16)$$

Finally, we can reconstruct the uniformly sampled sequence by taking the inverse transform of the obtained DFRFT $F^{\alpha}[m]$. It is easy to show that the result of (16) reduces to the result of [23] in the Fourier domain when $\alpha = \pi/2$.

3.2 Preferable reconstruction from non-uniform short samples by optimal angle and symmetric extensions

As shown in the results presented above, the uniformly sampled sequence can be reconstructed from non-uniform samples in the FRFD. In the reconstruction, the inverse transform of the obtained DFRFT $F^{\alpha}[m]$ is the most critical step. To reach better results in the reconstruction, we hope that the corresponding power spectrum is more concentrated on a few coefficients and there are few high-frequency contents in the FRFD.

First, we give the solution scheme of how to make the corresponding power spectrum more concentrated on a few coefficients. The Parseval relation and energy-preserving property can be viewed as consequences of the fact that the FRFT is based on a set of orthonormal basis functions [3]. Due to the energy-preserving property of the FRFT, the squared FRFT magnitude can be interpreted as the distribution of the signal's energy among the different chirps. From its discrete form, we can obtain the energy either from the finite sequence or from the DFRFT magnitude $|F^{\alpha}[m]|$. If we want to make the corresponding power spectrum more concentrated on a few coefficients, we can acquire the energy from the less samples of the DFRFT magnitude by considering the even symmetry property of the DFRFT magnitude, i.e. $|F^{\alpha}[m]| = |F^{\alpha}[N-m]|$. From (8), we can deduce that this sequence $f[n]\mathrm{e}^{j(1/2)\cot\alpha n^2 \Delta t^2}$ should be real. In this case, the relationship between $F^{\alpha}[m]$ and $F^{\alpha}[-m]$ is

$$F^{\alpha}[m] \mathrm{e}^{-j(1/2)\cot\alpha m^2 \Delta u^2} = (F^{\alpha}[-m] \mathrm{e}^{-j(1/2)\cot\alpha m^2 \Delta u^2})^*, \quad (17)$$

where the superscript * indicates the complex conjugate. Therefore, the choice of angle α is associated with the continuous-time signal $f(t)$ and the optimal angle can make the corresponding power spectrum more concentrate on a few coefficients.

Second, we give an explanation for the existed high-frequency contents in the FRFD and show an effective solution to this problem. In practice, the signals are of finite length. They should be periodically extended before being processed with the DFRFT. Unfortunately, this periodisation will cause severe discontinuities at the boundaries which may add substantial high-frequency contents in FRFS and lead to spectral leakage. The computation of the DFRFT for a finite sequence is in fact computing the FRFS of its periodically extended sequence. This conclusion is derived in the following section. As the periodisation of non-uniformly sampled signals and uniformly sampled signals work in a similar way, we only consider this problem for uniformly sampled signals. Without loss of generality, we suppose that the number of samples N is odd.

We consider the signal $f(t)$ which is bandlimited to $(-\Omega_{\alpha}, \Omega_{\alpha})$ in the αth FRFD. The continuous-time signal $f(t)$ can be the chirp

periodic signal $f_p(t)$ by sampling the FRFT of $f(t)$. Thus

$$f_p(t) = \mathrm{e}^{-j(t^2/2)\cot\alpha} \sum_{m=-\infty}^{\infty} f\left(t - m\frac{2\pi\sin\alpha}{\Delta u}\right) \mathrm{e}^{j(1/2)\cot\alpha(t-m(2\pi\sin\alpha/\Delta u))^2}. \tag{18}$$

Then, the FRFS of the periodic signal $f_p(t)$ is

$$f_p(t) = \mathrm{e}^{-j(1/2)\cot\alpha\cdot t^2} \sum_{m'=-(N-1)/2}^{(N-1)/2} F_{m'} \mathrm{e}^{-j(1/2)\cot\alpha(m'\Delta u)^2} \mathrm{e}^{j(1/\sin\alpha)m'\Delta u\cdot t}, \tag{19}$$

where $F_{m'}$ are the FRFS coefficients of $f_p(t)$. As there are N uniform samples in the replicated period $2\pi\sin\alpha/\Delta u$, the sampling interval Δt in the time domain is $\Delta t = 2\pi\sin\alpha/(N\Delta u)$. Here, the choice of the sampling rate meets the requirement of the sampling theorem in the FRFD, which will not result in aliasing effects. These will result in a sequence as follows

$$f_p[n] = \mathrm{e}^{-j(1/2)\cot\alpha\cdot(n\Delta t)^2} \sum_{m'=-(N-1)/2}^{(N-1)/2} F_{m'} \mathrm{e}^{-j(1/2)\cot\alpha(m'\Delta u)^2} \mathrm{e}^{j(2\pi/N)m'\cdot n}, \tag{20}$$

where $n = 0, 1, 2, \ldots, N-1$. As shown in the previous section, when the number of samples N is odd, the inverse DFRFT becomes

$$f[n] = \frac{1}{NA_\alpha} \mathrm{e}^{-(j/2)\cot\alpha n^2\Delta t^2} \sum_{m'=-(N-1)/2}^{(N-1)/2} \mathrm{e}^{-(j/2)\cot\alpha m'^2\Delta u^2} F^\alpha[m'] \mathrm{e}^{j(2\pi/N)n\cdot m'}. \tag{21}$$

Equation (21) is identical to (20) when N is odd by equating

$$F^\alpha[m'] = NA_\alpha \cdot F_{m'}. \tag{22}$$

From (22), the corresponding conclusion about the relationship between the DFRFT and the FRFS is deduced. The sequence obtained by extending samples periodically across boundaries often causes some discontinuities at the edges. However, these edge discontinuities will introduce spurious components into the corresponding power spectrum and even add substantial high-frequency contents in the obtained DFRFT, which will have a negative effect on the preferable reconstruction of a uniformly sampled sequence. It should be noted that the effect of discontinuity on short non-stationary sequences is more critical than on long sequences. Therefore, it is worthwhile to overcome the effect of discontinuity on short non-stationary sequences.

The symmetric extension method [24] has been shown to be an attractive solution to the above problem because these edge discontinuities in the circular implementations can be eliminated by transforming an extension of the input signal. We call it an extended sequence whole-sample symmetric (WS) if it is symmetric about one of its samples and half-sample symmetric (HS) if it is symmetric about a point halfway between two samples. The finite sequences based on WS and HS extensions result in $2N-1$ and $2N$ points, respectively. Two types of symmetric extensions are shown in Fig. 1. The discontinuity problem at the edges is prevented in the symmetric extensions followed by periodic extension. Considering the aliasing effect and the demand that the corresponding power spectrum should be more concentrated on a few coefficients, the proposed reconstruction method in this paper is more suitable for the effectively time and band limited signals in the αth FRFD. When the choice of the sampling rate meets the requirement of the sampling theorem in the FRFD, the symmetric extension is effectively free of aliasing effects. As a sequence, there will be few high-frequency contents in the reconstructed DFRFT of the finite sequence based on the WS extension or HS extension. Therefore, the optimal angle and

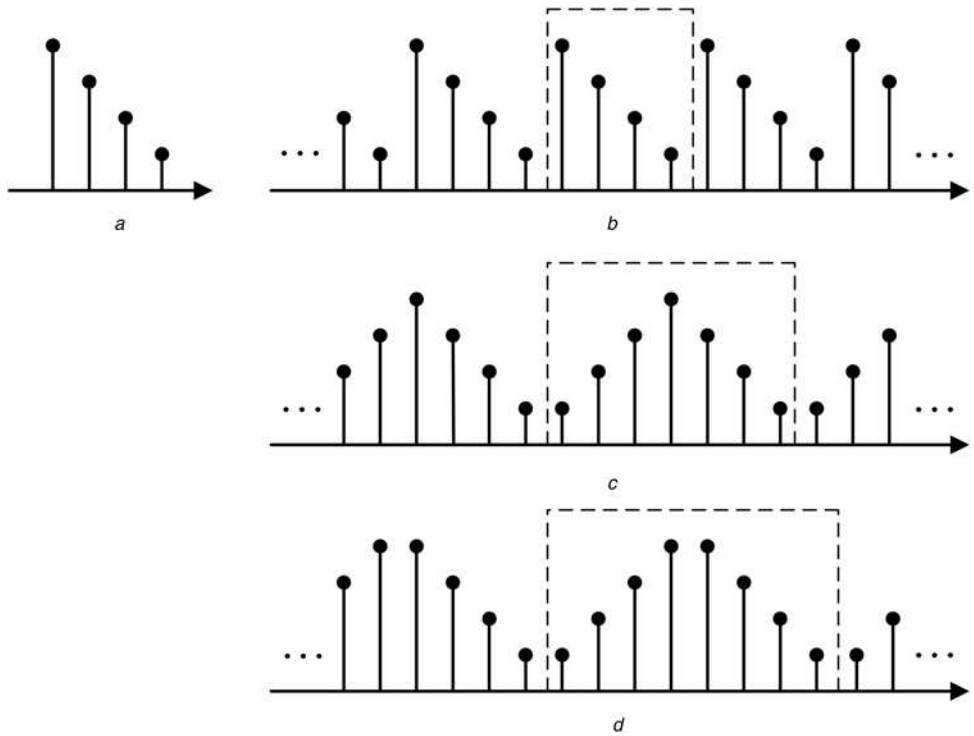

Fig. 1 *Two types of symmetric extensions*

a Initial sequence
b No extension followed by periodic extension
c WS followed by periodic extension
d HS followed by periodic extension

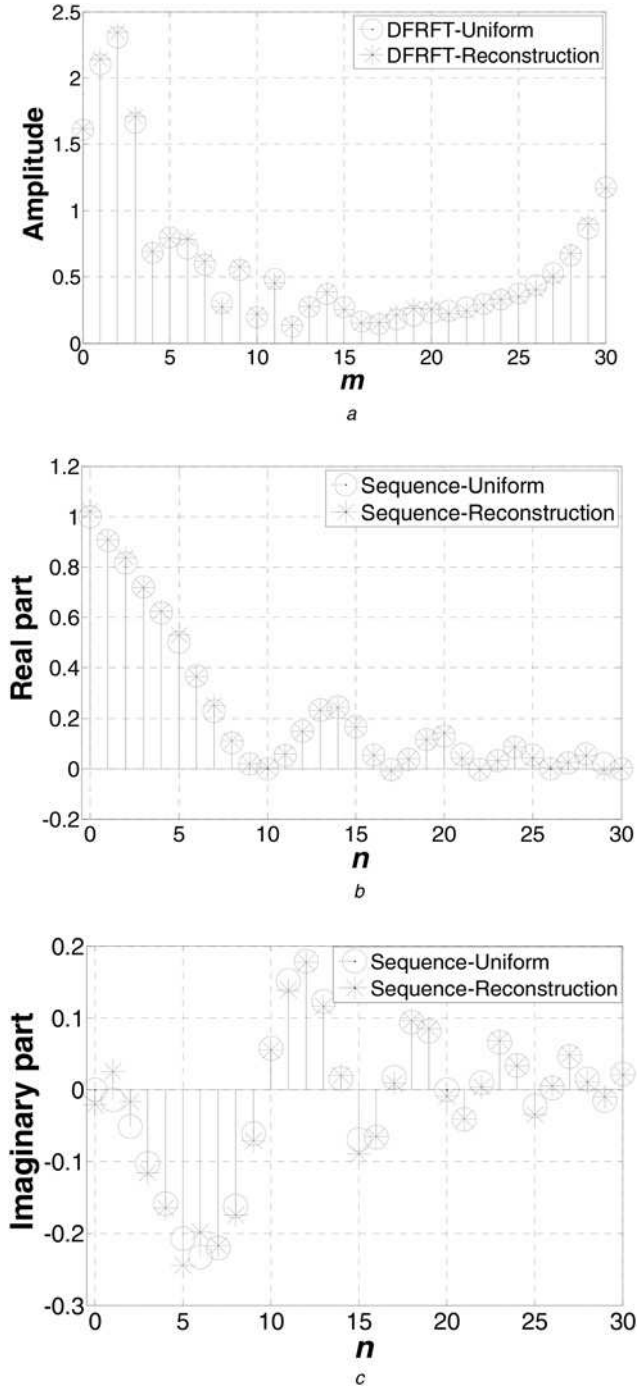

Fig. 2 *Reconstruction without symmetric extension when the angle is* $\alpha = 1.4483$

a Magnitude of the reconstructed DFRFT
b Real part of reconstructed uniformly sampled sequence
c Imaginary part of reconstructed uniformly sampled sequence

symmetric extensions are used in our reconstruction method for preferable reconstruction.

4 Simulation results and two applications of the proposed reconstruction method

In this section, some reconstruction examples of a uniformly sampled signal by the proposed method are demonstrated. The original continuous-time signal is a real exponent envelop function multiplied by a phase factor $\exp(-\mathrm{j}w_0t^2)$, i.e. $f(t) = \exp(-\mathrm{j}w_0t^2 - w_1t)\cos(w_2t^2 + w_2t) \cdot u(t)$, where $w_0 = w_2 = 0.005\pi$, $w_1 = 0.1$ and $u(t)$ is a unit step function. We suppose that the expected ideal sequence $f[n]$ is sampled uniformly at $t = n\Delta t$, and the discrete-time signal $\tilde{f}[n]$ is sampled non-uniformly at $t = (n + a_n)\Delta t$, where Δt is the sampling interval and a_n are sampling time offsets. We choose $\Delta t = 1$ and a_n to satisfy the statistically independent zero-mean Gaussian distribution. Here, the selection of the sampling interval meets the requirement of the sampling theorem in the FRFD. The standard deviations are chosen as 0.01, 0.02, 0.04 and 0.08. Since $\exp(-3) \simeq 0$, $f[n]$ and $\tilde{f}[n]$ are approximated as a finite signal in the interval [0, 30], and they can be numerically simulated on a computer. The number of samples is $N = 31$.

Due to the fact that a discontinuity problem exists in the periodically extended version of a uniformly sampled sequence and a non-uniformly sampled sequence, WS and HS extensions of the sequence are considered in preferable reconstruction. The finite

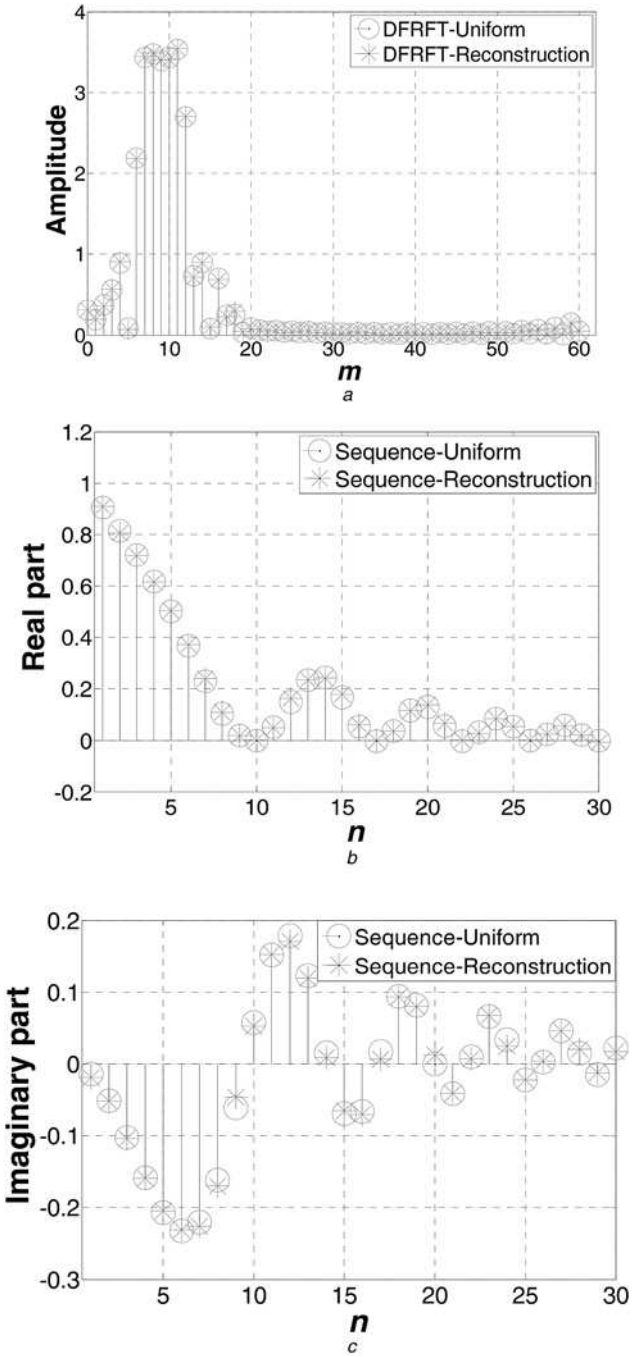

Fig. 3 *Reconstruction with WS extension when the angle is* $\alpha = 1.5394$

a Amplitude of reconstructed DFRFT
b Real part of a reconstructed uniformly sampled sequence
c Imaginary part of a reconstructed uniformly sampled sequence

IET Signal Process., 2016, Vol. 10, Iss. 2, pp. 140–149

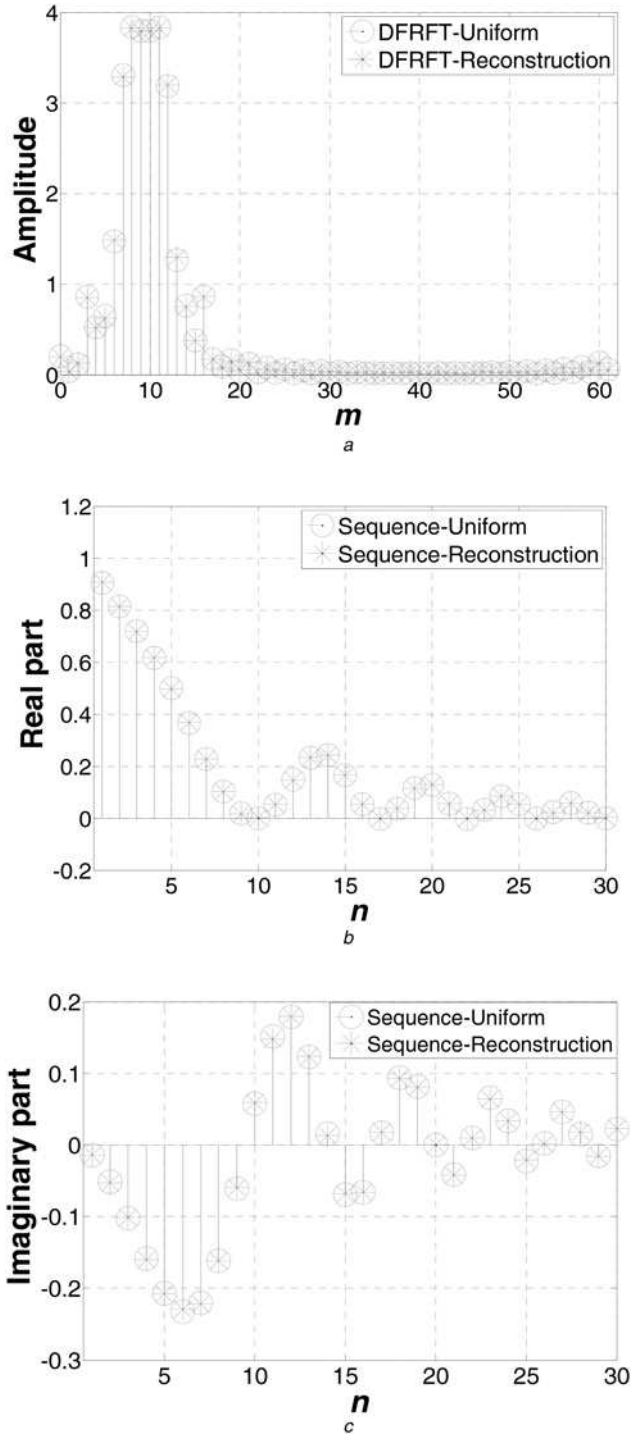

Fig. 4 *Reconstruction with HS extension when the angle is $\alpha = 1.5394$*

a Amplitude of the reconstructed DFRFT
b Real part of a reconstructed uniformly sampled sequence
c Imaginary part of a reconstructed uniformly sampled sequence

sequences based on WS and HS extensions result in 61 and 62 points, respectively. The average signal-to-noise ratio (SNR) is used to evaluate the advantages of two types of symmetric extensions in our work. A total of 500 trials are performed at each standard deviation. The average SNR is computed using the following method

$$\text{average SNR (in dB)} = 10\log_{10} \frac{\text{signal power}}{(1/500)\sum_{m=1}^{500}[\text{noise power in each trial}]}, \quad (23)$$

where signal power is $(1/N)\sum_{n=0}^{N-1} f[n]^2$ and the noise power in each trial is $(1/N)\sum_{n=0}^{N-1}\{f[n]-\hat{f}[n]\}^2$. In (23), $f[n]$ is the ideal uniformly sampled sequence, and $\hat{f}[n]$ is the reconstructed uniformly sampled sequence by taking the inverse transform of $F^{\alpha}[m]$ in each trial.

4.1 Reconstruction of the uniformly sampled sequence without symmetric extension

In this simulation, the standard deviation of the sampling time offsets is chosen as 0.04. Then, the reconstructed uniformly sampled sequence and the amplitude of the reconstructed DFRFT without symmetric extension in the αth FRFD are obtained. From the results of the reconstructed DFRFT shown in Fig. 2*a*, we can clearly find that there are substantial high-frequency contents in the αth FRFD because of the discontinuity problem. For $\alpha = 1.4483$, the average SNR is 28.6934 dB, and the effect of the reconstruction is not very well. It is obvious that both the reconstructed uniformly sampled sequence and the amplitude of the reconstructed DFRFT shown in Fig. 2 do not match the uniformly sampled counterparts at some points very well.

4.2 Reconstruction of the uniformly sampled sequence with WS and HS extensions

To overcome the discontinuity problem and reduce substantial high-frequency contents in the αth FRFD, the WS and HS extensions are considered in our reconstruction. Here, the standard deviation of the sampling time offsets is chosen as 0.04, and the reconstructed uniformly sampled sequence and the amplitude of the reconstructed DFRFT with two types of symmetric extensions in the αth FRFD are obtained. In our simulation, the angle is set as $\alpha = 1.5349$. The simulation results of the reconstruction with WS and HS extensions are plotted in Figs. 3 and 4, respectively. Moreover, the corresponding average SNRs are 38.2490 and 48.5289 dB. It is clear from Figs. 3*a* and 4*a* that these substantial high-frequency contents in the αth FRFD are greatly reduced. Consequently, from Figs. 3 and 4, the real part and imaginary part of the reconstructed uniformly sampled sequence are

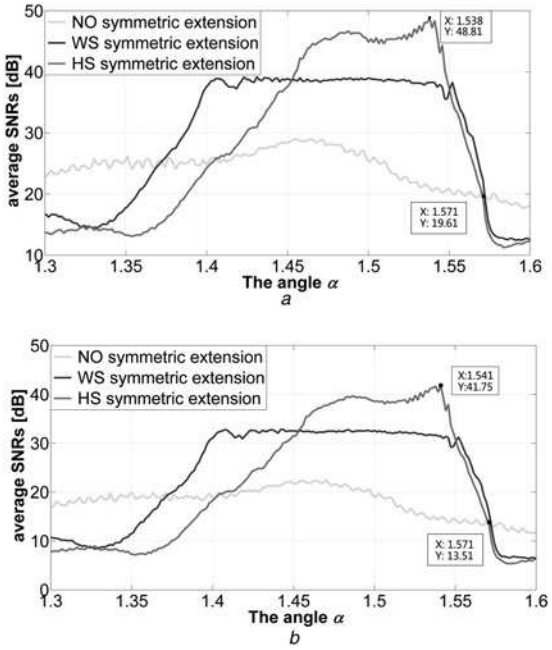

Fig. 5 *Curves of the average SNRs against the angle of the DFRFT when the standard deviations of the sampling time offsets are chosen as*

a 0.04
b 0.08

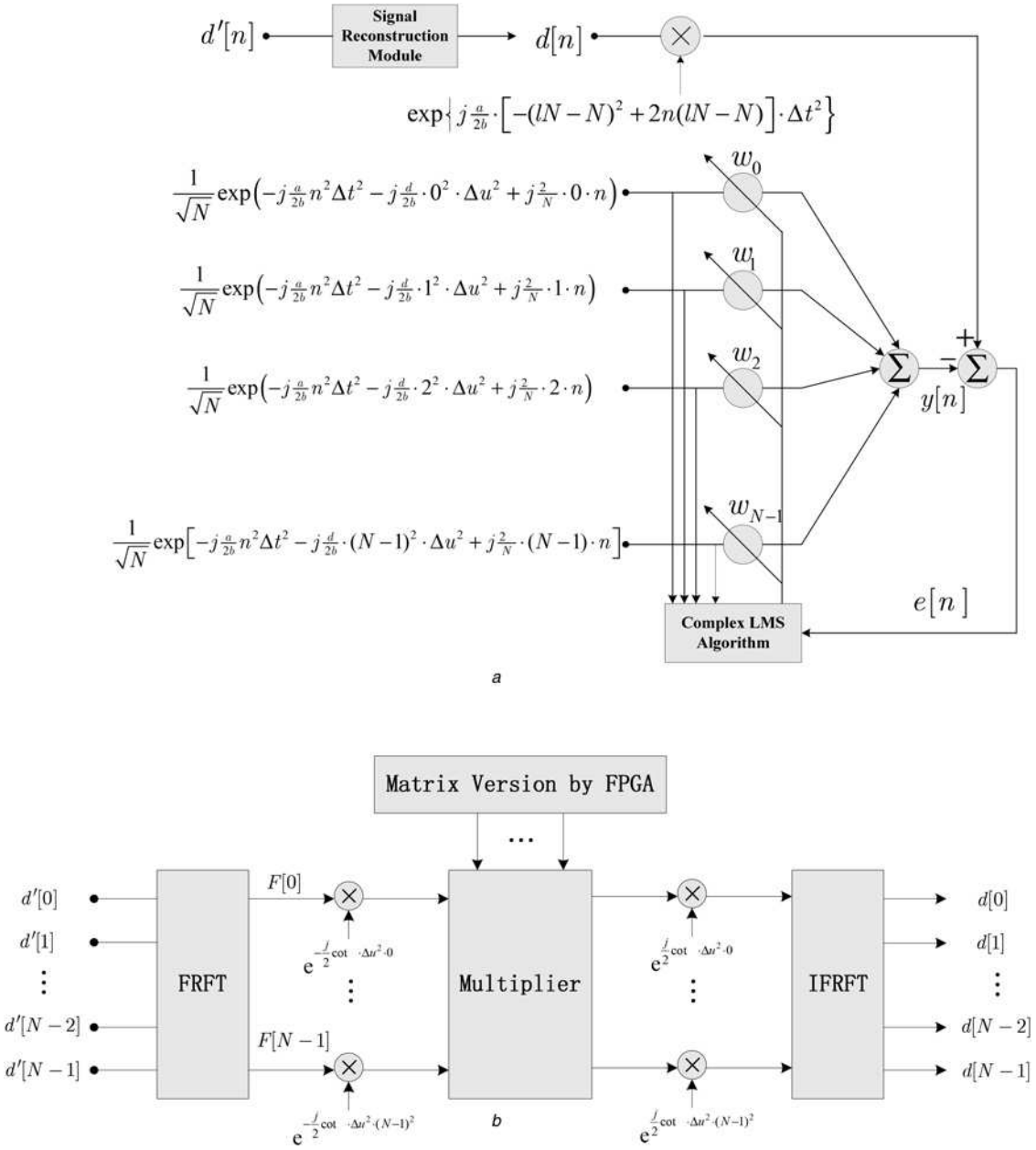

Fig. 6 *Structure implementation of the DLCT computation using the adaptive filtering system*

a Structure implementation of the DLCT computation using the adaptive method when the input is a non-uniformly sampled signal
b Details of the signal reconstruction module

approximately equal to the ideal uniformly sampled sequence $f[n]$, which imply the advantages of our proposed method. Specifically, we can find that the HS extension performs better than the WS extension with a 10 dB advantage in the average SNR in our simulation.

4.3 Average SNRs against the angle of the DFRFT

It is well-known that the FRFT can be interpreted as a rotation by an angle α in the time–frequency plane, so the selection of the angle should be considered to obtain the preferable reconstruction. In this subsection, we exploit the relationship between the average SNRs and the angle α of the DFRFT in detail. The standard deviation of the sampling time offsets can be chosen as 0.01, 0.02, 0.04 and 0.08, respectively. Moreover, the range of the angle is $1.3 \leq \alpha \leq 1.6$ and the step of the angle is set as $0.001\pi/2$ in our simulation.

Fig. 5 shows the average SNRs against the angle of the DFRFT under three conditions: no symmetric extension, WS and HS extensions, where the standard deviations of the sampling time offsets are chosen as 0.04 and 0.08, respectively. Note that for $\alpha = \pi/2$, the DFRFT degenerates to the discrete FT. In this case, the average SNRs for no symmetric extension, WS and HS extensions are nearly the same (we especially denote this phenomenon in the figure). However, the effects of the reconstruction with WS and HS extensions outperform those without symmetric extension in a range of the angle $\alpha = [1.46, 1.55]$ because there is nearly a 10–24 dB advantage in average SNRs with WS and HS extensions over the case without symmetric extension. When the standard deviations of the sampling time offsets are chosen as 0.01 and 0.02, the curves of the average SNRs are similar to Figs. 5*a* and *b*. It is interesting to note that the HS extension performs best, which is reflected in the second subsection as a special case. According to the definition of the FRFT, the matched-angle is $\alpha_0 = \operatorname{arc}\cot(-\mu_0)$ when the chirp rate of a chirp signal is μ_0. In our simulation, the chirp rate of the envelop of the original

continuous-time signal is $u_0 = -2\omega_0$, so the matched-angle is $\alpha_0 = 1.5394$ theoretically. From Fig. 5, it is shown that the positions of the maximum value of the average SNRs are 1.538 and 1.541, respectively, which are very close to the theoretical value and imply the correctness of the proposed method. Thus, we can confirm the optimal angle for preferable reconstruction.

4.4 Two applications of the proposed reconstruction method

4.4.1 DLCT computation by the proposed reconstruction method and the adaptive method: The LCT is a three-parameter linear integral transform that describes the effect of quadratic phase systems on a wavefield. The LCT generalises many transforms, such as the FT, FRFT and Fresnel transform. These integral transforms are of great importance in electromagnetic, acoustic and other wave propagation problems where they represent the solution of the wave equation under a variety of circumstances. The details regarding the properties of LCT can be referred in [25, 26]. Understanding the LCT can provide more insights into its applications and carry the knowledge gained from one subject to others. Due to the importance of the LCT, the discrete linear canonical transform (DLCT) has become an important issue. The various definitions and implementations of the DLCT have been derived. The DLCT computation by the adaptive method has been presented in [27], including the approach of computing the block DLCT using the adaptive least-mean-square (LMS) algorithm. Since the adaptive algorithm can automatically adjust for possible errors, the appearing error in the computation process of the DLCT is attenuated when it propagates over time.

In the DLCT computation by the adaptive LMS algorithm, a uniform sampling signal is used in the adaptive filter system. Due to the imperfect sampling timebase of interleaving/multiplexing techniques, the exact uniform sampling sequence cannot be obtained in practical applications. The non-uniform samples cannot be used directly in the DLCT computation by the adaptive method or result in incorrect performance. At the same time, to minimise the error, the number of iterations and the computation complexity in the inherent parallel structures will greatly increase when the adaptive filter is adjusted according to the error signal generated by using the non-uniform sampling sequence. Therefore, based on the proposed reconstruction method in this paper, we can implement the DLCT computation by using the non-uniform samples and the adaptive LMS algorithm. Namely, the DLCT computation by the adaptive LMS algorithm can be accomplished after the uniformly sampled sequence is reconstructed from the non-uniform samples. Here, the structure implementation of the DLCT computation using the adaptive filtering system is shown in Fig. 6. We suppose that the input sequence $d'[n]$ is the non-uniformly sampled signal $\tilde{f}[n]$, and the output sequence of the signal reconstruction module $d[n]$ is the uniformly sampled signal $f[n]$.

The DLCT computation by the reconstructed uniformly sampled sequence and adaptive filtering technique has an inherent parallel structure that makes it suitable for efficient VLSI implementation. To illustrate that the reconstruction method works well with the DLCT computation, a numerical example of the DLCT computation by the proposed reconstruction method and the adaptive LMS algorithm is demonstrated. For illustration purposes, we only select the reconstructed uniformly sampled sequence based on the HS extension. Using the above results in Fig. 4, we consider the DLCT of the signal with parameters $(a, b, c, d) = (3, 1, 1/2, 1/2)$. The DLCT of a uniformly sampled signal, reconstructed sampled signal and non-uniformly sampled signal computed by the adaptive LMS algorithm are shown in Fig. 7, where the standard deviations of the sampling time offsets are chosen as 0.04 and 0.08, respectively. The average SNR of the DLCT can also be used to evaluate the advantages of the reconstruction method. From the simulation results in Fig. 7, we find that the DLCT of a non-uniformly sampled signal $\tilde{f}[n]$ does not match exactly with the DLCT of the expected ideal sequence $f[n]$. In this case, the corresponding average SNR is

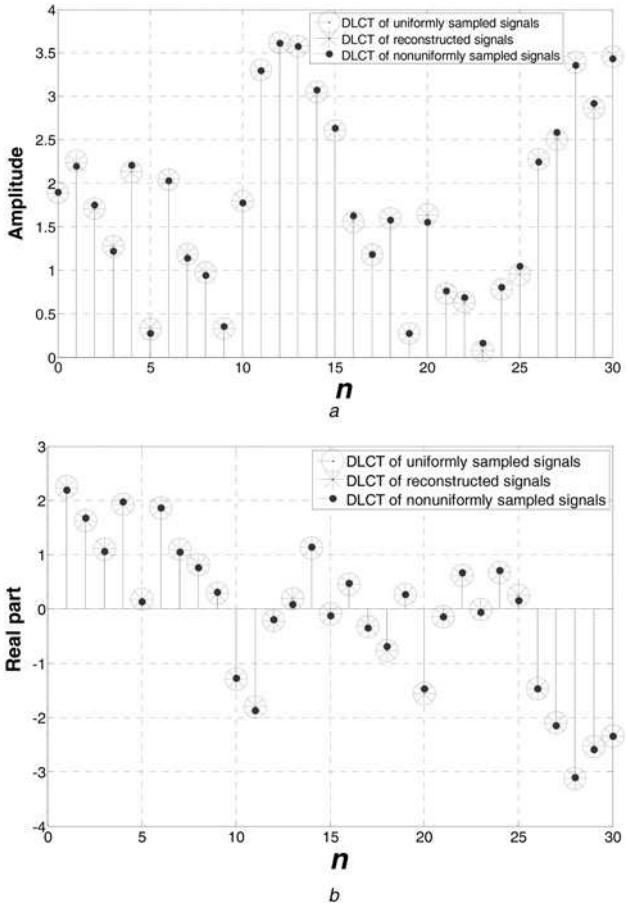

Fig. 7 *DLCT of a uniformly sampled signal, reconstructed sampled signal and non-uniformly sampled signal computed by the adaptive LMS algorithm*

a Amplitude

b Real part results of the DLCT with parameters (3, 1, 1/2, 1/2) computed by the adaptive method

26.7750 dB. Namely, if we do not use the reconstruction method, error exists in the DLCT computation by the adaptive method. After reconstructing the uniformly sampled signals from the non-uniform samples used by the proposed reconstruction method, the DLCT of the reconstructed uniformly sampled signal shown in Fig. 7 is nearly equal to the DLCT of uniform samples and the corresponding average SNRs is 34.8092 dB, which will reduce the error in the parallel structure implementation of the DLCT computation by the adaptive method.

4.4.2 Application of the reconstruction technique in frequency-modulated continuous wave (FMCW) synthetic aperture radar (SAR) signal processing: A high-resolution wide-swath image with a mini-sized system is becoming more important in military monitoring and small-scale earth observation applications. As one of the new radar systems, the FMCW SAR offers a lightweight, high-resolution and cost-effective imaging sensor of high resolution [28–30]. Moreover, high-resolution and wide-swath SAR images can be obtained by multichannel sampling.

Table 1 System parameters

carrier frequency	9.6 GHz
pulse repeat frequency	100 Hz
velocity	250 m/s
subaperture distance	4/3 m
number of subapertures	3
minimum slant	30 km
synthetic aperture time	2 s
synthetic aperture length	500 m

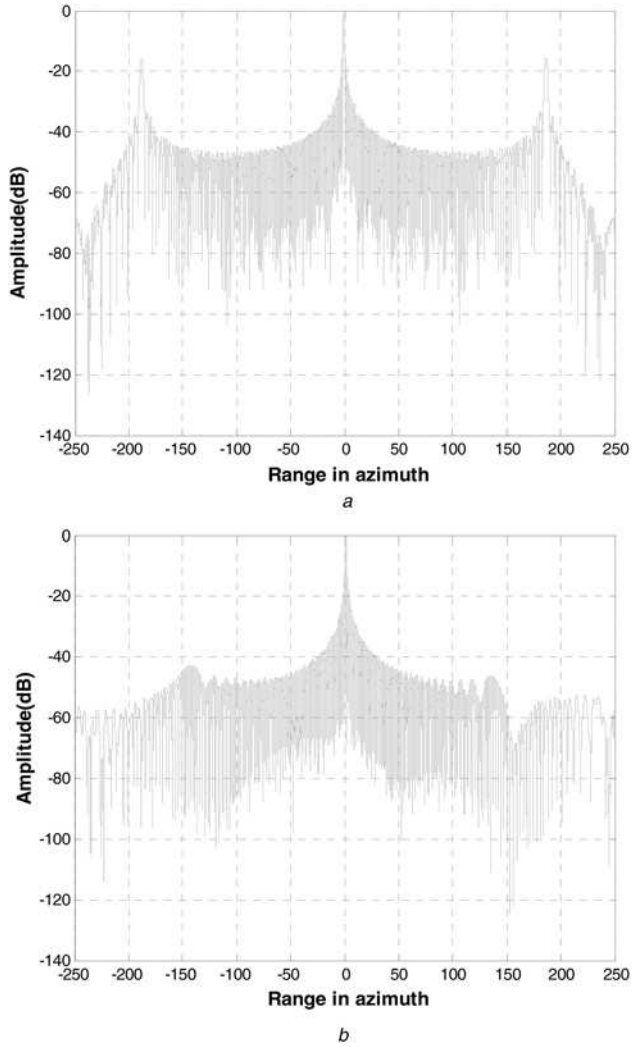

Fig. 8 *Simulation results after matched filtering in the time domain*

a Signal is directly dealt
b Signal is reconstructed by the proposed method

Here, the number of subapertures is chosen as M. However, a non-optimum pulse-repetition frequency (PRF) is associated with a non-uniform spatial sampling in azimuth. Since the subaperture distance $\triangle x$ and the specific PRF are fixed in a single-platform system, the theoretical platform velocity v of uniform sampling can be constrained to be a constant value. Namely

$$v = \frac{1}{2} M \cdot \triangle x \cdot \mathrm{PRF} \tag{24}$$

If the platform velocity deviates from the theoretical speed, the azimuth signal of the FMCW SAR becomes the non-uniformly sampled signal, which will lead to some ambiguous targets in the azimuth detection. To eliminate the effects, we need to reconstruct the uniformly sampled signals from the non-uniformly sampled signals. Perfect reconstruction of the digital spectrum from non-uniformly sampled signals has already been presented by Jenq [14]. Moreover, Gebert and co-workers [28] have developed a reconstruction algorithm based on the filter group algorithm. However, the energy focusing ability is not greatly reflected in the process of analysis. According to the signal model of the FMCW SAR system, the echo from a ground moving target can be regarded approximately as a chirp signal. Hence the FRFT is a way to concentrate the energy of a chirp signal, the FRFT presents a potentially effective technique for moving target detection. Fortunately, the relationship between uniformly sampled signals and non-uniform samples in the FRFD has been derived and the uniform sampling sequence can be reconstructed from the non-uniform echo sampling signals in this paper. Therefore, we can eliminate the effects of the ambiguous targets by considering the advantages of the FRFT and improve the detection performance of the FMCW SAR.

Assume that the radar platform flies along a straight line with an altitude and a velocity. The antennas are located along the flight direction, where one antenna is both transmitting and receiving and the other antennas are receiving. The relevant system parameters are summarised in Table 1. Then, a numeric demonstration of the reconstructed signal is given. When a rigid selection of the PRF may be in conflict with the timing diagram for some incident angles, the theoretical platform velocity of the uniform sampling is changed and the echo of the FMCW SAR in the azimuth is a non-uniformly sampled signal. If we deal directly with it as a uniformly sampled signal, there are two false targets in the azimuth detection, as shown in Fig. 8*a*. Based on the proposed reconstruction method with an HS extension in this paper, the uniformly sampled signal can be reconstructed from the non-uniform samples provided that the matched-angle is chosen correctly. After matched filtering in the time domain, two false targets shown in Fig. 8*a* are eliminated successfully. From Fig. 8*b*, it is shown that the detection performance of the FMCW SAR is greatly improved.

5 Conclusion

This paper describes the reconstruction of a uniformly sampled signal from non-uniform short samples with WS and HS extensions in the FRFD. First, the relationship between the DFRFT of a uniformly sampled sequence and the DFRFT of a non-uniformly sampled sequence is derived. For preferable reconstruction, WS and HS extensions are used to reduce some substantial high-frequency contents of the obtained DFRFT in the FRFD. The performance of the reconstruction is represented by the average SNRs, which are computed and compared in a range of the angle. Simulation results show that the reconstruction with WS and HS extensions outperform the reconstruction without symmetric extension. Specifically, the HS extension performs the best. Moreover, we provide two applications of the proposed reconstruction method. The proposed reconstruction method improves the theories of non-uniform sampling and promotes the applications for the reconstruction of non-stationary discrete-time signals in the FRFD.

6 Acknowledgments

This work was supported in part by the National Natural Science Foundation of China under Grants Nos. 61201354, 61571042, 61331021 and 61421001, and by the Beijing Higher Education Young Elite Teacher Project (YETP1221).

7 References

1 Ozaktas, H.M., Zalevsky, Z., Kutay, M.A.: 'The fractional Fourier transform with applications in optics and signal processing' (Wiley Press, New York, 2001, 1st edn.)
2 Cabañas-Molero, P., Martínez-Muñoz, D., Vera-Candeas, P., *et al.*: 'Voicing detection based on adaptive aperiodicity thresholding for speech enhancement in non-stationary noise', *IET Signal Process.*, 2014, **8**, (2), pp. 119–130
3 Almeida, L.B.: 'The fractional Fourier transform and time–frequency representations', *IEEE Trans. Signal Process.*, 1994, **42**, (11), pp. 3084–3091
4 Lee, S.H., Park, J.B., Choi, Y.H.: 'Blind spot reduction in wavelet transform-based time–frequency domain reflectometry using Gaussian chirp as mother wavelet', *IET Signal Process.*, 2014, **8**, (7), pp. 703–709
5 Mei, L., Chenlei, L., Shuqing, Z.: 'Joint space-time-frequency method based on fractional Fourier transform to estimate moving target parameters for multistatic synthetic aperture radar', *IET Signal Process.*, 2013, **7**, (1), pp. 71–80
6 Zhu, M., Li, B.Z., Yan, G.F.: 'Aliased polyphase sampling associated with the linear canonical transform', *IET Signal Process.*, 2012, **6**, (6), pp. 594–599
7 Pei, S.C., Yeh, M.H., Luo, T.L.: 'Fractional Fourier series expansion for finite signals and dual extension to discrete-time fractional Fourier transform', *IEEE Trans. Signal Process.*, 1999, **47**, (10), pp. 2883–2888

8 Clemente, C., Soraghan, J.J.: 'Range Doppler and chirp scaling processing of synthetic aperture radar data using the fractional Fourier transform', *IET Signal Process.*, 2012, **6**, (5), pp. 503–510
9 White, P.R., Locke, J.: 'Performance of methods based on the fractional Fourier transform for the detection of linear frequency modulated signals', *IET Signal Process.*, 2012, **6**, (5), pp. 478–483
10 Xia, X.G.: 'On bandlimited signals with fractional Fourier transform', *IEEE Signal Process. Lett.*, 1996, **3**, (3), pp. 72–74
11 Tao, R., Zhang, F., Wang, Y.: 'Sampling random signals in a fractional Fourier domain', *Signal Process.*, 2011, **91**, (6), pp. 1394–1400
12 Tarczynski, A., Allay, N.: 'Spectral analysis of randomly sampled signals: suppression of aliasing and sampler jitter', *IEEE Trans. Signal Process.*, 2004, **52**, (12), pp. 3324–3334
13 Dumitrescu, B., Bregović, R., Saramäki, T.: 'Design of low-delay nonuniform oversampled filterbanks', *Signal Process.*, 2008, **88**, (10), pp. 2518–2525
14 Jenq, Y.C.: 'Perfect reconstruction of digital spectrum from nonuniformly sampled signals', *IEEE Trans. Instrum. Meas.*, 1997, **46**, (3), pp. 649–652
15 Erseghe, T., Kraniauskas, P., Cariolaro, G.: 'Unified fractional Fourier transform and sampling theorem', *IEEE Trans. Signal Process.*, 1999, **47**, (12), pp. 3419–3423
16 Pei, S.C., Ding, J.J.: 'Closed-form discrete fractional and affine Fourier transform', *IEEE Trans. Signal Process.*, 2000, **48**, (5), pp. 1338–1353
17 Tao, R., Li, B.Z., Wang, Y.: 'Spectral analysis and reconstruction for periodic nonuniformly sampled signals in fractional Fourier domain', *IEEE Trans. Signal Process.*, 2007, **55**, (7), pp. 3541–3547
18 Wei, D.Y., Ran, Q.W., Li, Y.M.: 'Multichannel sampling and reconstruction of bandlimited signals in the linear canonical transform domain', *IET Signal Process.*, 2011, **5**, (8), pp. 717–727
19 Wei, D.Y., Li, Y.M.: 'Reconstruction of multidimensional bandlimited signals from multichannel samples in linear canonical transform domain', *IET Signal Process.*, 2014, **8**, (6), pp. 647–657
20 Maravic, I., Vetterli, M.: 'Sampling and reconstruction of signals with finite rate of innovation in the presence of noise', *IEEE Trans. Signal Process.*, 2005, **53**, (8), pp. 2788–2805
21 Jenq, Y.C.: 'Digital spectrum of a nonuniformly sampled two-dimensional signal and its reconstruction', *IEEE Trans. Instrum. Meas.*, 2005, **54**, (3), pp. 1180–1187
22 Harish, V., Sommen, P., Prabhu, K.M.M.: 'Perfect reconstruction of uniform samples from K-th order nonuniform samples', *Signal Process.*, 2011, **91**, (11), pp. 2677–2684
23 Park, S.W., Hao, W.D., Leung, C.S.: 'Reconstruction of uniformly sampled sequence from nonuniformly sampled sequence from symmetric extension', *IEEE Trans. Signal Process.*, 2012, **60**, (3), pp. 1498–1501
24 Martucci, S.A.: 'Symmetric convolution and the discrete sine and cosine transforms', *IEEE Trans. Signal Process.*, 1994, **42**, (5), pp. 1038–1051
25 Pei, S.C., Ding, J.J.: 'Closed-form discrete fractional and affine Fourier transforms', *IEEE Trans. Signal Process.*, 2000, **48**, (5), pp. 1338–1353
26 Tao, R., Song, Y.E., Wang, Z.J., *et al.*: 'Ambiguity function based on the linear canonical transform', *IET Signal Process.*, 2012, **6**, (6), pp. 568–576
27 Zhang, F., Tao, R., Wang, Y.: 'Discrete linear canonical transform computation by adaptive method', *Opt. Express.*, 2013, **21**, (15), pp. 18138–18151
28 Krieger, G., Gebert, N., Moreira, A.: 'SAR signal reconstruction from non-uniform displaced phase center sampling'. Proc. IEEE Int. Geosci. Remote Sens. Symp., Anchorage, AK, USA, 2004, vol. 3, pp. 1763–1766
29 Liu, Y., Deng, Y.K., Wang, R., *et al.*: 'Model and signal processing of bistatic frequency modulated continuous wave synthetic aperture radar', *IET Radar Sonar Navig.*, 2012, **6**, (6), pp. 472–482
30 Jia, G.W., Chang, W.G.: 'Study on the improvements for the high-resolution frequency modulated continuous wave synthetic aperture radar imaging', *IET Radar Sonar Navig.*, 2014, **8**, (9), pp. 1203–1214